PREPRINT UCRL-78186

CONF-760539--1

Lawrence Livermore Laboratory

A HIGH-INTENSITY, SUBKILOVOLT X-RAY CALIBRATION FACILITY

R. W. Kuckuck, J. L. Gaines, and R. D. Ernst

May 6, 1976

This paper was prepared for submittal to the ERDA Symposium on X- and Gamma-Ray Sources and Applications, Ann Arbor, Michigan, May 19-21, 1976.

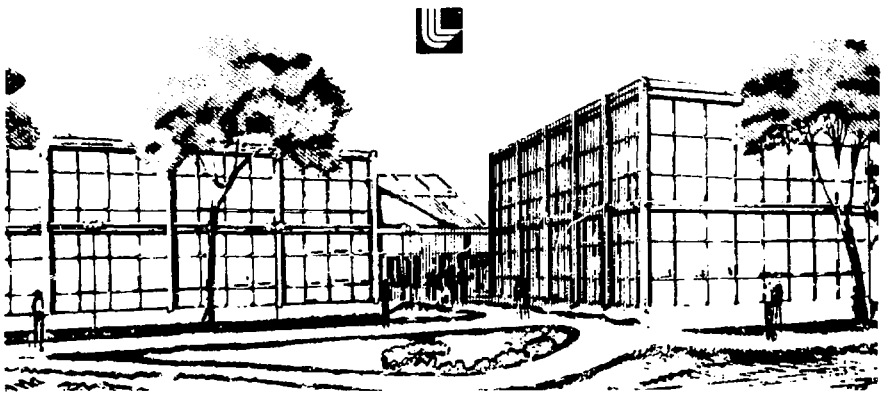

A HIGH-INTENSITY, SUBKILOVOLT X-RAY CALIBRATION FACILITY*

R. W. Kuckuck, J. L. Gaines, and R. D. Ernst
Lawrence Livermore Laboratory, University of California
Livermore, California, 94550

Summary

A high-intensity subkilovolt x-ray calibration source utilizing proton-induced inner-shell atomic fluorescence of low-Z elements is described. The high photon yields and low brensstrahlung background associated with this phenomenon are ideally suited to provide intense, nearly monoenergetic x-ray beams. The proton accelerator is a 3 mA, 300 kV Cockroft-Walton using a conventional rf hydrogen ion source. Seven remotely-selectable targets capable of heat dissipation of 5 kW/cm^2 are used to provide characteristic x-rays with energies between 100 and 1000 eV. Source strengths are of the order of 10^{13}-10^{14} photons/sec. Methods of reducing spectral contamination due to hydrocarbon build-up on the target is discussed. Typical x-ray spectra (Cu-L, C-K and B-K) are shown.

Introduction

Considerable need has arisen for the development of well-calibrated x-ray detectors capable of detecting photons with energies between 100 and 1000 electron-volts. This energy region is of significant interest since the x-ray emission from high-temperature (kT ~ 0.5 keV), laser produced plasmas is predominantly in this range. For this application interest is mainly on fast, current-mode detectors capable of responding linearly to the intense x-ray bursts produced by these sources. These bursts are characterized by durations of approximately 100 ps and peak photon intensities of ~ 10^{25} photons/ster-sec. Typical detectors used in these measurements include semiconductor detectors, scintillator photodiode detectors and photoelectric diodes.[1] Since these detectors have sensitivities of the order of 10^{-17}-10^{-22} coul/keV, it is clear that, in order to be accurately calibrated in the current mode, intense sources of monoenergetic x-rays must be available.

One obvious source of monoenergetic subkilovolt x-rays is the characteristic line emission from inner-shell atomic fluorescence of low-Z elements. This fluorescence can be induced by various types of exciting radiations, i.e., photons, electrons, or ions. However, the fluorescence yield for low-Z elements is quite low and intense ionization sources are needed to obtain useful x-ray yields. While photon or electron excitation methods are common x-ray generation techniques, both approaches exhibit a serious disadvantage, namely lack of spectral purity due to photon scattering and/or bremsstrahlung continuum backgrounds superimposed on the characteristic line emissions. To avoid this particular difficulty, x-ray production via ion bombardment has become a phenomenon of significant recent interest. The high yields and low bremsstrahlung backgrounds associated with this process are ideally suited to the above detector calibration objectives.

Numerous investigators have reported x-ray yields from charged particle bombardment for many different species of target and projectile ions and over a wide range of incident particle energies.[2] Consequently, much of the physical principles of the excitation and emission processes are well understood. In view of this understanding, and with the above-stated detector-calibration objectives in mind we have developed a calibration facility at LLL utilizing characteristic x-ray production in elemental targets via Coulomb excitation from proton bombardment. While heavier ions may provide greater photon yields for specific cases in which the energy level of the projectile and target atoms overlap, proton excitation provides a consistently high yield for general excitation of a wide variety of target material. Also, in considering the dependence of x-ray yield and of secondary electron bremsstrahlung production upon the incident proton energy it appeared practical to base the facility around a low-energy (300 kV) accelerator.

Facility Description

The LLL calibration facility consists of a charged particle accelerator, x-ray target chamber, photon monitoring system, experimental detector chamber and crystal diffractometer (Figure 1). Figure 2 shows a schematic layout of the x-ray generation and detection portion of the system. The accelerator power supply is based on conventional Cockcroft-Walton voltage multiplying principles and was designed and fabricated at LLL.[3] It has an oscillation frequency of 100 kHz and maximum load capability of 5 mA and 300 kV. The voltage is applied across a conventional accelerating column and the proton beam is magnetically analyzed and delivered to the x-ray target through electrostatic quadrupole focusing elements. The accelerating column and beam drift tubes are maintained at a pressure of ~ 2 x 10^{-6} Torr during full beam loading by two 1500 ℓ/sec oil-diffusion pumps. Vacuum integrity throughout this section is achieved using Viton O-ring seals.

Fig. 1. Photograph of the LLL extreme low-energy x-ray facility. Vacuum chamber in foreground is the x-ray chamber. Accelerator beam tube is seen to the upper left. The two chambers in the upper right are the experimental detector chamber and the crystal diffractometer chamber, respectively.

*Work performed under the auspices of the U.S. Energy Research and Development Administration under contract No. W-7405-Eng-48.

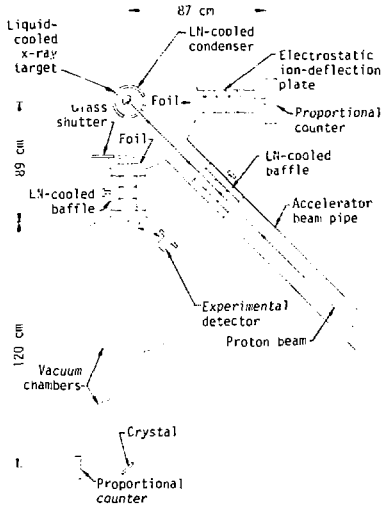

Fig. 2. Schematic illustration of the x-ray production and detection portion of the facility.

The proton beam is provided by a standard rf ionization source and beam currents of ~ 2.5 mA have been delivered on target in a spot size of less than 5 mm diameter. Smaller spot sizes are possible but under such conditions target heat loads are excessive. The accelerator is also capable of accelerating heavier ions or electrons with only minor system modifications.

Three high-vacuum stainless steel experimental chambers are mounted in series at the end of the accelerator drift tube (Figures 1 and 2). These chambers have metal vacuum seals and are evacuated to pressures of 10^{-7}-10^{-8} Torr using 250 ℓ/sec sputter-ion pumps. Isolation of these chambers from the poorer vacuum environment of the accelerator beam tube is achieved by a low-conductance (6 ℓ/s), double-walled, LN-cooled cold trap mounted in the beam pipe at the entrance to the target chamber. This trap is designed to reduce hydrocarbon buildup on the x-ray target which, as will be discussed later, is a serious detriment to spectral purity in subkilovolt x-ray generators.

The x-ray target has two primary features: a) heat dissipation of 5 kW/cm^2, and b) capability of remote selection of one of several different target materials, and hence, characteristic photon energies. Seven target materials (Cu, Fe, Cr, Ti, C, B, Be) are deposited on the flat machined surface of a high-purity Cu cylinder to thicknesses ranging from 3 to 5 mg/cm^2 (Figure 3).

A 50 percent mixture of ethylene glycol and water is flowed through the cylinder past the back of the targets for temperature control. The flow system is designed not only to dissipate up to 5 kW/cm^2 of

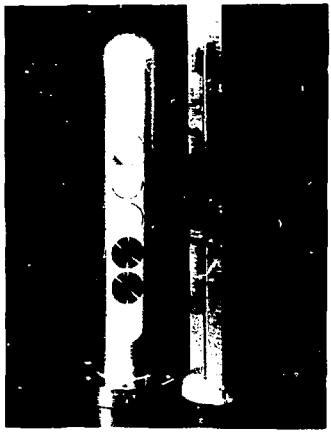

Fig. 3. X-ray targets plated on high-purity Cu cooling probe.

target heat during beam loading conditions but also to maintain the target temperature at 115° C during beam-off conditions. The latter is achieved by heating the liquid and is an attempt to further reduce condensation of hydrocarbon contaminants on the target face. The liquid is flowed at 6 ℓ/min, through a closed-loop pump and heat exchanger system and is nozzled to pass the back of the targets with a turbulent velocity of 7.5 m/sec.

As a final step in minimizing carbon buildup a double-walled, LN-filled cylinder is mounted around the targets to serve as a hydrocarbon condenser. The target and condenser are electrically isolated to permit beam current measurements and to allow bias voltage suppression of secondary electron emission from the target. The target assembly is vertically driven by a remotely-controlled stepping motor and will automatically position any pre-selected target in the proton beam. Figures 4 and 5 show the target assembly mounted to the chamber lid.

The target chamber geometry is designed to allow continuous monitoring of the x-ray flux with a proportional counter during calibration of an experimental detector. Both the experimental detector and the proportional counter monitor are mounted symmetrically at an angle of 135° with respect to the incident proton beam direction (Figure 2). The x-ray emission is found to be isotropic only for very smooth targets (polished so that average peak-to-valley surface roughness is less than 0.05 μm). Targets with rougher surfaces, e.g., 8 μm, exhibit highly nonisotropic emission and preclude use of the monitor detector output to derive the flux level incident on the experimental detector. Consequently, since target surface damage and roughness can readily occur at high current loads, it is necessary to frequently recheck isotropy using a second proportional counter in place of the experimental detector.

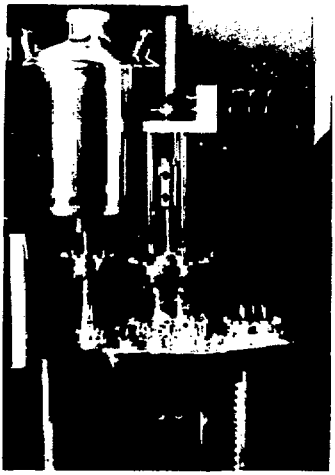

Fig. 4. Photograph of remotely switchable target assembly mounted on vacuum chamber lid.

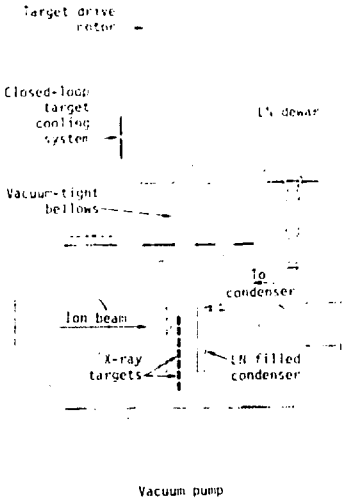

Fig. 5. Schematic illustration of remotely switchable target assembly mounted on vacuum chamber lid.

The proportional counters are side-window, cylindrical, gas-flow counters with 2.5 cm inside diameters, 0.25 mm diameter tungsten anode wires and 0.25 mm diameter, 85 μg/cm² Formvar entrance windows. Their operating characteristics for detecting Cu-L (930 eV) and C-K (280 eV) x-rays are shown in Table I.

	Cu-L (930 eV)	C-K (280 eV)
Counter gas:	P-10	He-isobutane
Gas pressure:	760 Torr	760 Torr
Anode voltage:	1600 V	1150 V
Window transmission: (measured)	0.75	0.76
Counting efficiency: (calculated)	1.0	0.76
Energy resolution: (measured)	325 eV	112 eV

Table I. Operating characteristics of the gas-flow proportional counters.

The counter window transmissions are measured for each photon energy of interest and the counter efficiencies are calculated using published mass absorption coefficients for P-10 and helium-isobutane gases.[7] The output pulses of the proportional counter are amplified and analyzed using conventional techniques.

The experimental detectors are mounted on a rotary table in a second vacuum chamber connected to the target chamber and can be remotely rotated onto the 135° x-ray beam axis symmetrical with the monitor detector (Figure 2). Various thin foils are placed in front of both detectors, experimental and monitor, and serve several purposes. First, in some cases, they are opaque and shield the detectors from visible and infrared fluorescent and incandescent radiation emitted from the hot target. Optical pyrometer measurements have shown a carbon target to stabilize at approximately 1900° C during loading with a 2 mA proton beam. Second, they are thick enough to stop backscattered protons and hydrogen atoms. Buck et. al.[8] have shown that for these proton energies (300 keV) a large fraction of the backscattered projectiles are neutralized. Consequently, any attempt to remove recoil particles from the x-ray flux by electrostatic deflection techniques would only be partially successful. Hence, absorbing foils are necessary. Finally, in some cases the foils selectively absorb photons characteristic of carbon contamination on the target surface. This requires matching the x-ray absorption cross-section of the foil with the characteristic photon energies of carbon and of the target material to maximize the x-ray flux at the detector. All three functions are considered in selection of the proper foil-target combinations. For example, 600 μm/cm², opaque, carbon foils are used with a carbon target and 700 μg/cm², opaque Be foils are used with a copper target.

A third vacuum chamber mounted behind the experimental detector chamber (Figure 2) will house a crystal diffractometer and gas-flow proportional counter for high-resolution spectrum analysis.

Facility Performance

The facility is designed for nominal operation at 3 mA beam current and 300 kV accelerating potential.

Table II lists the x-ray source strengths anticipated for these operating parameters. To date, however, the accelerator has been routinely operated at only 1 mA and 200 kV and has been used to generate characteristic x-rays in solid B, C and Cu targets. Results have been encouraging. Figures 6 and 7 show pulse-height spectra obtained from the monitor proportional counter for Cu-L and C-K rays, respectively. Although filtered from the spectrum shown in Figure 6 by a thin Be foil in front of the detector, x-rays due to carbon contamination of the Cu target have been apparent. However, no special precautions were taken to reduce this contamination and significant improvement is anticipated with the incorporation of continuously heated targets and the LN$_2$-cooled condenser associated with the multiple target assembly. This assembly will be installed on the system shortly. The spectrum shown in Figure 8 was obtained by subtracting the C-K component from a composite carbon-boron spectrum emitted by a carbon-contaminated boron target.

Target	Photon Energy (eV)	Approximate Source Strength (Photons/sec)
Be-K	110	4×10^{13}
B-K	185	4×10^{13}
C-K	280	4×10^{13}
Ti-L	450	1×10^{13}
Cr-L	570	1×10^{13}
Fe-L	704	1×10^{13}
Cu-L	930	2×10^{13}

Table II. X-ray source strengths for 3 mA proton beam current and 300 kV accelerating potential.

Fig. 6. Pulse height spectrum due to Cu-L (930 eV) x-rays detected by thin-window proportional counter. See Table I for counter operating characteristics.

Table III lists the x-ray source intensities and thick-target photon yields obtained from the present single-target (1 mA, 200 kV) data. These are in excellent agreement with published results.[4] It should be noted that for a given target material, the L-shell photon yield is many orders of magnitude greater than the K-shell yield[4] and hence, the latter may be ignored with respect to the spectral purity of the x-ray source. Note that these source strengths will increase by a factor of ten when the accelerator is operated at its design level of 3 mA and 300 kV.

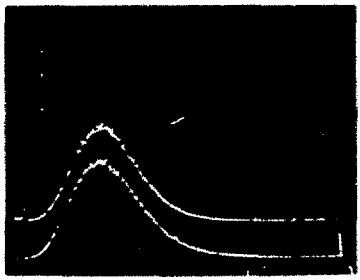

Fig. 7. Pulse height spectra due to C-K (280 eV) x-rays detected by two thin-window proportional counters. Counters were mounted simultaneously in the monitor and experimental detector positions (see Figure 2) to demonstrate isotropy of the x-ray emission. See Table I for counter operating characteristics.

Fig. 8. Pulse height spectrum due to B-K (185 eV) x-rays detected by thin-window proportional counter. Carbon contamination of the target was significant and Boron spectrum was obtained by subtracting C-K component from composite spectrum.

	Cu-L (930 eV)	C-K (280 eV)
Source strength (photons/sec)	1.9×10^{13}	6.5×10^{13}
Thick-target yield (photons/proton)	3×10^{-7}	1×10^{-6}

Table III. Source strengths and proton-induced thick-target x-ray yields obtained from experimental data (proton beam current: 1 mA, accelerating voltage: 200 kV). See Table II for anticipated source strengths when accelerator is operated at full design level of 3 mA and 300 kV.

Acknowledgements

We would like to acknowledge the contributions of H. E. Smith, R. Steele and R. Ullman for designing the accelerator power supply, accelerator control systems and multiple-target assembly, respectively. Also we wish to thank D. Nelson, M. Griffin and J. Arguello for their efforts in fabricating and assembling the apparatus.

References

1. Gaines, J. L., Kutkuck, R. W., and Ernst, R. D., paper presented at ERDA Symposium on X- and Gamma Ray Sources and Applications, May 19-21, 1976, Ann Arbor, Michigan.

2. Garcia, J. D., Fortner, R. J., and Kavanagh, T. M., Rev. Mod. Phys. 45 (1973) 111.

3. Reginato, L. L., and Smith, B. H., paper presented at the Particle Accelerator Conference, March 10-1[illegible], 196[illegible], Washington, D. C. Also LLL report [illegible]-117[illegible], March 2, 1965.

4. [illegible], et. al., Norelco Reporter [illegible], No. [illegible] (19[illegible]) [illegible].

5. Buck, T. M., Wheatley, G. H., and Feldman, L. C., Surface Science 35 (1973) [illegible].

6. [illegible], et. al., Japanese Journal of Applied Physics [illegible] (197[illegible]) 1297-130[illegible].